Mathematical Modelling and Simulation of Combustion and Heat Transfer in a Spark Ignition Engine Running On Ethanol-Petrol Blends

Nwaji, G.N., Eze, D., Nwufo, O., Onwachu, C.C. and Ofong, I.

Abstract

The mathematical model of combustion and heat transfer processes in a spark ignited internal combustion engine has been developed from first principle. The combustion process is based on a two-dimensional thermal theory of combustion such that the prediction of combustion temperature distribution and heat flux within the charged mixture contained in the cylinder during the combustion phase of the engine operation from -30° before top dead centre to +30° after top dead centre crank angles can be predicted. The model has been parameterized using E10, E20 and E30 ethanol-petrol blended fuels and implemented on a computer simulation code based on Finite Element numerical scheme. The study revealed maximum temperature at top dead centre and steep temperature gradients axially from top dead centre to bottom dead centre and radially to the cylinder walls where it is lowest for the combustions of the three blends. Heat transfer, dominantly convective, within the cylinder from the burning gases increases radially from top dead centre to the chamber walls.

Keywords: IC Engine; Combustion; Model; Heat Transfer; Spark Ignition; Ethanol-Petrol Blend; Numerical Simulation.

1 Introduction

Spark ignition (SI) engines are known for high specific power and energy resulting from energy release from combustion of fuel in the engine. Developing in-depth understanding of the in-cylinder combustion process is required in the optimization of the overall performance of internal combustion engines. The overall process of converting the thermal energy of the fuel into mechanical energy of the reciprocating components has intrinsic thermodynamics and heat transfer constraints, which might be wrongly interpreted as losses. However, the actual thermal loss in the combustion chamber is the heat flow through the walls, which is predominantly influenced by forced convection. Engine power and efficiency have become the major issues that automotive engine designers are currently concentrating efforts on. Ethanol-petrol blends, though reputed for low energy content in comparison with their pure petrol counterparts, have been reported to possess higher volumetric efficiency, higher research octane number, faster rate of combustion and lesser sensitivity. These qualities have conferred on the blended fuels improved power output, enhanced compression ratio, and less prone to knock. The effect of the blends on the performance of engines and pollutant emissions as well as environmental sustainability has become a subject of increased interest today. The presence of oxygen within the ethanol fuel molecule and the contribution of its faster flame speed results in enhanced combustion initiation and stability as well as improved engine efficiency [1]. Apart from the inherent potential to increase petrol octane rating, ethanol-petrol blends have been reported to reduce the emission of volatile organic compounds by 20–40% and consequently yield an average reduction of 17% in the ozone formation potential [2]. Mahmoud and Ahmed [3] modeled the combustion process of an engine running on gasoline (100%) and different gasoline-ethanol blends (95% gasoline + 5% ethanol; 90% gasoline + 10% ethanol). The model was purely thermodynamic employing first law of thermodynamics, energy equations, equation of state and mass fraction burned. The model results closely matched the results of experiment obtained a four-stroke spark ignition engine. They reported that the model predicted brake specific fuel consumption and thermal efficiency to within 3% and 4% accuracy respectively. In order to develop a deeper understanding of in-cylinder heat transfer, [4], studied the spatial effect of heat transfer on engine performance using Reynolds analogy. They carried out measurements on the piston and cylinder head during combustion using a new heat flux sensor due to high cost of commercial heat flux sensor. They investigated the effect of the propagating flame front on convective heat transfer in the system. Spitsov [5] theoretically and experimentally studied heat transfer in cylinder head of swirl-chamber compression ignition (CI) engine. The temperature gradient normal to the head was higher than that along the wall surface. Gustof and Hornik [6] modeled the temperature distribution in the wet cylinder sleeve of a turbocharged diesel engine using a two zone combustion approach and finite element method. They concluded that it is possible to

predict the temperature distribution on the individual surfaces of the cylinder during the combustion process. The loss of energy through the walls during compression and combustion strokes of a spark ignition engine has been investigated by [7]. This was informed by the fact that energy loss estimation during these two strokes provides better information on the system dynamics and operation during combustion. Belal et al [8] modeled in-cylinder gas motion and combustion in a direct injection diesel engine with bowl-in piston. They presented a detailed turbulent combustion model including spray formation, delay period, chemical kinetics and onset of ignition. The model predicted the in-cylinder flow patterns, combustion process and combustion species but however over predicted the peak of cylinder pressure by 6% for different engine loads. Ajayi and Nwaji [9] carried out a numerical study of in-cylinder temperature distribution and heat transfer in a compression ignition engine running on n-Dodecane, a conventional diesel fuel. They adopted a thermal theory approach and reported temperature profiles along the radial, axial and wall linings. Also, wall linings are influenced greatly by the prevailing temperature in the combustion chamber, and for proper material selection for such intricate parts, knowledge of the temperature distribution and heat transfer during in-cylinder combustion is imperative. According to Nwufo et al [10], ethanol blends improve power output, operates in engines with high compression ratio and improve efficiency due to their high rate of vaporization, increased research octane number and higher laminar flame speed, respectively. Hence, ethanol blends improve the in-cylinder combustion process and are superior to pure petrol. Therefore, this work is premised on the need to extend this approach to spark ignited engines running on alternative fuels, specifically ethanol-petrol blends.

2 Model formulation

In order to formulate the model of the in-cylinder combustion process, it was assumed that the combustion process occurred in two dimensions, material and fluid properties are temperature dependent, internal heat generation occurs in the combustion chamber, and combustion is time-variant and turbulent. The above assumptions were made to make possible the simplification of combustion process for easy representation of its dynamics with generated mathematical equations.

The general energy equation of combustion based on heat conduction can be represented as [11]:

$$\rho c_p \frac{\partial T}{\partial t} = \nabla.(k\nabla T) + Q\dot{R}_f \quad (1)$$

For a constant thermal conductivity of the reacting species, Eq. 1 reduces to:

$$\rho c_p \frac{\partial T}{\partial t} = k\nabla^2 \mathrm{T} + Q\dot{R}_f \quad (2)$$

According to Heywood [12], $Q\dot{R}_f$ is the heat energy generated by the reacting species in the cylinder during the combustion process, in which Q is the fuel calorific value and $\dot{R}_f$ is the rate of disappearance of unburned fuel mixture expressed as:

$$\dot{R}_f = A\rho^2 \omega_f^a \omega_{ox}^b \exp(-\frac{E_a}{R_u T}) \quad (3)$$

Where A is the frequency factor of the reacting species, E_a is the activation energy of the reacting species, ω_f and ω_{ox} are the unburned fuel and oxidizer mass fractions respectively while a, b are constants which can take 1 or 0.5.

Therefore, (2) can be written employing the divergence of temperature gradient for the in-cylinder geometry and substituting (3), as:

$$\rho c_p \frac{\partial T}{\partial t} = k\frac{\partial^2 T}{\partial r^2} + \frac{1}{r}\frac{\partial T}{\partial r} + \frac{\partial^2 T}{\partial z^2} + QA\rho^2 \omega_f^a \omega_{ox}^b \exp(-\frac{E_a}{R_u T}) \quad (4)$$

The finite time steps (∂t) can be converted to crank angle steps ($\partial\theta$) using the relation:

$$\partial t = \frac{\partial \theta}{\omega} \quad (5)$$

Where ω is the angular velocity of the engine given as:

$$\omega = 2\pi N \quad (6)$$

On appropriate substitutions, (4) becomes:

$$\frac{\partial T}{\partial \theta} = \frac{\alpha}{2\pi N}\left(\frac{1}{r}\frac{\partial T}{\partial r} + \frac{\partial^2 T}{\partial r^2} + \frac{\partial T^2}{\partial z^2}\right) + \frac{QA\rho^2 \omega_f^a \omega_{ox}^b \exp(\frac{-E_a}{R_u T})}{2\pi N \rho C_p} \quad (7)$$

2.1 Heat transfer model

According to Stone [13], Heat transfer from combustion products occur by convection and radiation, but in spark-ignited engines convective exchange is predominant. Hence,

$$\dot{q} = h(T_g - T_w) \quad (8)$$

From the relation of Nusselt Number expressed as:

$$h = c\frac{k}{x}\left(\frac{\rho u x}{\mu}\right)^z \quad (9)$$

Since the details of the fluid motion are not of paramount importance, the characteristic length (x) can be taken to be the engine bore(B) while the characteristic velocity (u) is assumed to be the instantaneous piston speed (s_p) Hence, (9) becomes:

$$h = c\frac{k}{B}\left(\frac{\rho S_p B}{\mu}\right)^z \quad (10)$$

Therefore, the rate of convective heat transfer from the combustion products is given as:

$$\dot{q} = c\frac{k}{B}\left(\frac{\rho S_p B}{\mu}\right)^z (T_g - T_w) \quad (11)$$

The instantaneous piston speed can be correlated as:

$$S_p = \omega R(\frac{\sin 2\theta}{2n} + \sin\theta) \quad (12)$$

Where ω is the angular velocity of the crank-connecting rod mechanism given as:

$$\omega = 2\pi N \quad (13)$$

And N is the engine speed, θ is the crank angle, L is the connecting rod length, R the crank radius and n is the

connecting rod-to-crank radius ratio; c and z are constants, which can take values from the range: c = 0.3-0.5, z = 0.6-0.9. The cylinder wall temperature can be evaluated using Gill's correlation, given as [14].

$$T_w = T_g(\gamma_v)^{r-1} \quad (14)$$

Where T_g is the combustion temperature of the burnt gases and γ_v is the engine compression ratio, given as,

$$\gamma_v = \frac{V_s+V_c}{V_c} \quad (15)$$

And V_s and V_c are the swept and clearance volumes of the engine, respectively.

The temperature during combustion in a cylinder can be correlated with mass flow rate (ṁ), density (ϱ) and kinematic viscosity ($\dot{v}$) of the working fluid (fuel) by using the Hagen-poiseuille equation as given by [15]

$$T_g = \frac{\dot{v}\dot{m}8L}{\rho R_u \pi R^4} \quad (16)$$

2.2 Chemical species model

Combustion is assumed to be stoichiometric and reaction rate infinitely fast, with all the fuel injected vaporizing and combustion products formed. According to Nwufo et al [10], for the stoichiometric combustion of a bio-ethanol-petrol blend, the general expression for complete combustion in air is given as:

$$\%C_{\alpha 1}H_{\beta 1} + \%C_{\alpha 2}H_{\beta 2}O_{\gamma} + (\alpha_t + \frac{\beta_t}{4} - \frac{\gamma}{2})(O_2 + \frac{79}{21}N_2) \rightarrow \alpha_t CO_2 + \frac{\beta_t}{2}H_2O + (\alpha_t + \frac{\beta_t}{4} - \frac{\gamma}{2})\frac{79}{21}N_2 \quad (17)$$

Where,

$$\alpha_t = \%\alpha_1 + \%\alpha_2 \quad (18)$$

$$\beta_t = \%\beta_1 + \%\beta_2 \quad (19)$$

The combustion mixture species specific heat capacity c_p, density ϱ, and species mole fraction x and mass fractions ω can be obtained, respectively as [16], [17].

$$c_p = \sum X_i c_{pi} \quad (20)$$

$$\rho = \sum X_i \rho_i \quad (21)$$

$$\omega = \frac{M_i n_i}{\sum_{j=1}^{N} M_1 n_1} \quad (22)$$

The model engine is a G200 IMEX single cylinder 4-stroke engine with specification given in table 1, while the constants for the simulation of heat transfer in the cylinder are given in table 2. Three blends of ethanol-petrol, namely, E10 (10% ethanol, 90% petrol), E20 (20% ethanol, 80% petrol) and E30 (30% ethanol, 70% petrol) have been simulated. The fuel parameters, density ϱ, specific heat capacity c_p, heating value (Q), activation energy E_a, pre-exponential factor A, fuel mass fraction ω_f, oxidizer mass fraction ω_{ox}, fuel temperature at ambient conditions T_f, and adiabatic flame temperature T_{ad}, calculated from (17)-(22) are given in table 3.

Table 1: Model engine parameters [10]

PARAMETER	SPECIFICATION
Cylinder Bore, B	0.068m
Engine Stroke, L	0.045m
Engine capacity	0.000163m^3
Piston displacement	0.000196m^3
Compression ratio	8.5:1
Maximum horse power	6.5Hp/3600rpm
Maximum torque	13Nm/2500rpm
Fuel consumption	0.389kg/KWhr
Crank radius, R	0.062m
Connecting Rod Length, l	0.21m
Engine swept volume, Vs	0.000173m^3
Clearance volume, V_C	0.0000231m^3
Expansion index, γ	1.33

Table 2: Model constants

R_u (KJ/kmolK)	σ (W/m^{2}K^4)	a	b	c	z	β	μ	r_o	L	θ_o
8.1345	5.6661×10^{-8}	0.5	0.5	0.5	0.9	0.075	1.7227*10^{-8}	0.034	0.045	180^o

Table 3: Ethanol-Fuel Blends Parameters [17]

Fuel type	ϱ (kg/m^3)	C_P (kJ/kgK)	Q (kJ/kmol)	E_a (kJ/kmol)	A (cm^3/kmol)	ω_f	ω_{ox}	T_f	T_{ad}
E10	14.809	1.035	44,220	80964	1.5*10^{12}	0.072	0.716	300	2431*
E20	16.122	1.038	42,080	78888	1.5*10^{12}	0.074	0.678	300	2424*
E30	17.945	1.042	40,480	76812	1.5*10^{12}	0.077	0.64	300	2400

* [18]

3 Results and discussion

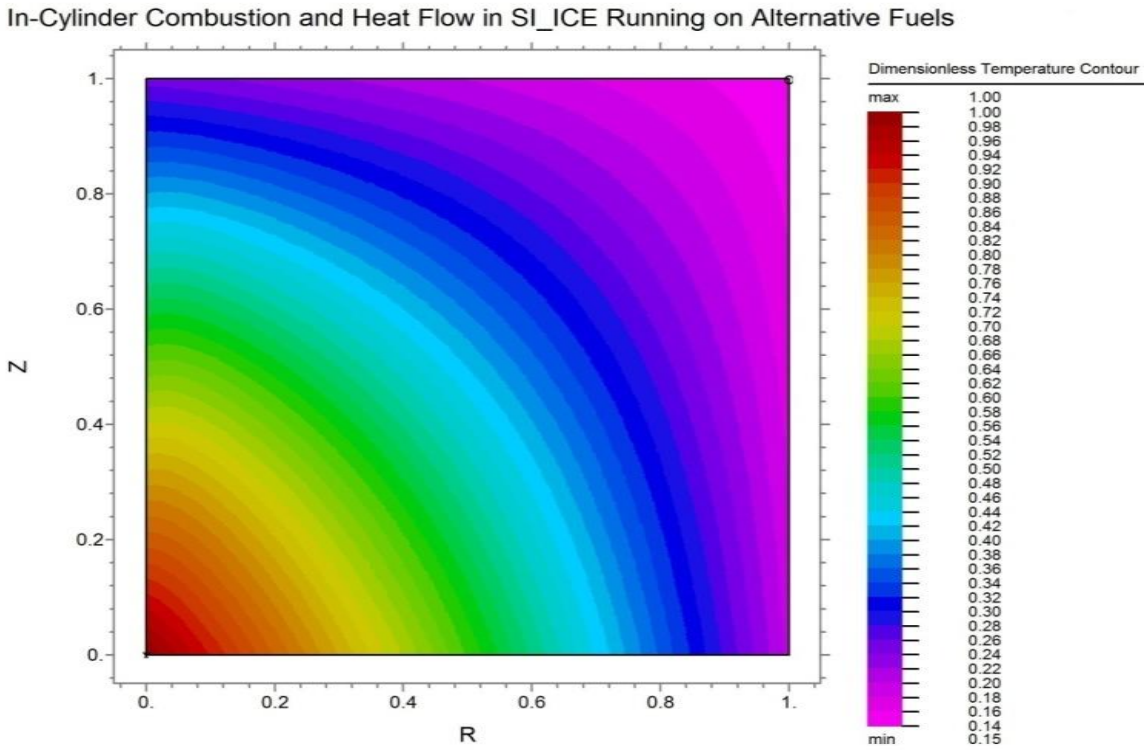

Fig. 1: Contour plot of dimensionless in-cylinder temperature for E10, E20 and E30 blends

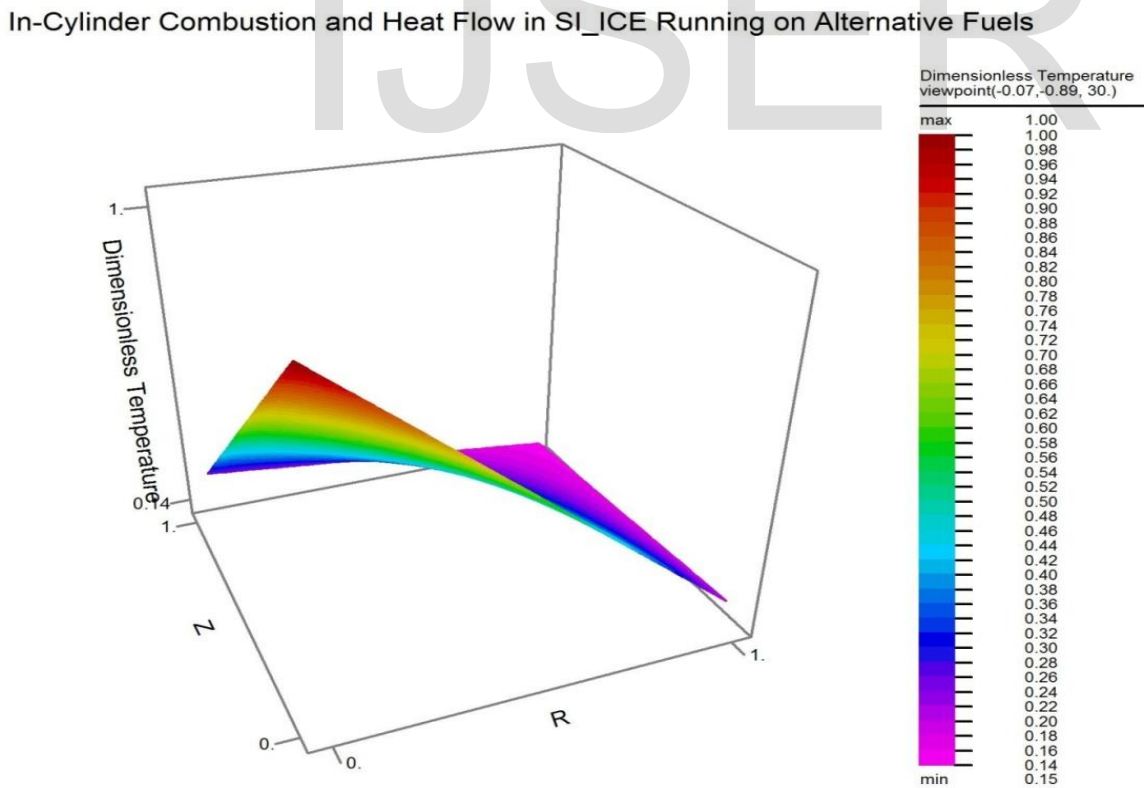

Fig 2: Fig 2: Surface plot of dimensionless in-cylinder temperature for E10, E20 and E30 blends

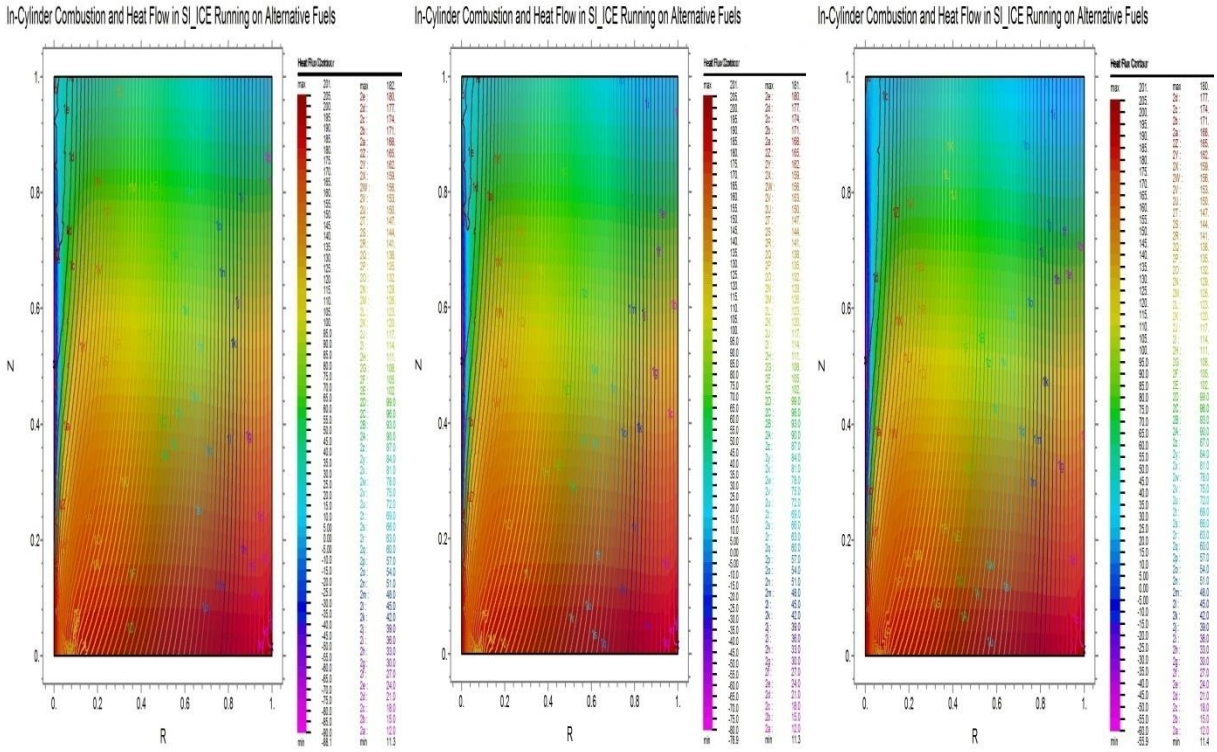

E10 E20 E30

Fig 3: Contour plot of in-cylinder heat flux for E10, E20 and E30 blends

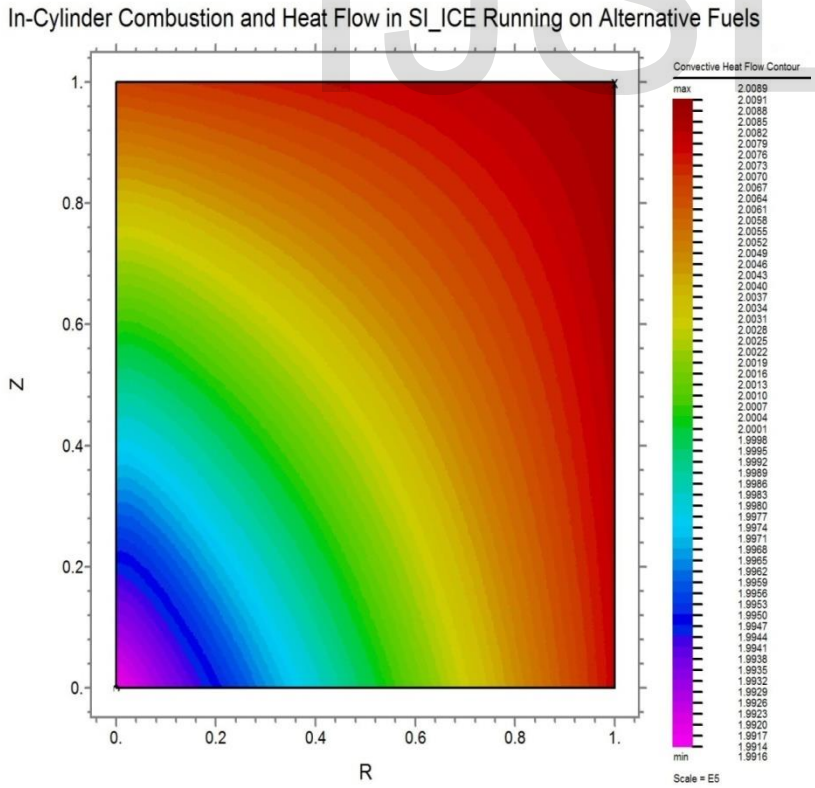

Fig 4a: Contour plot of in-cylinder convective heat flow for E10 blend

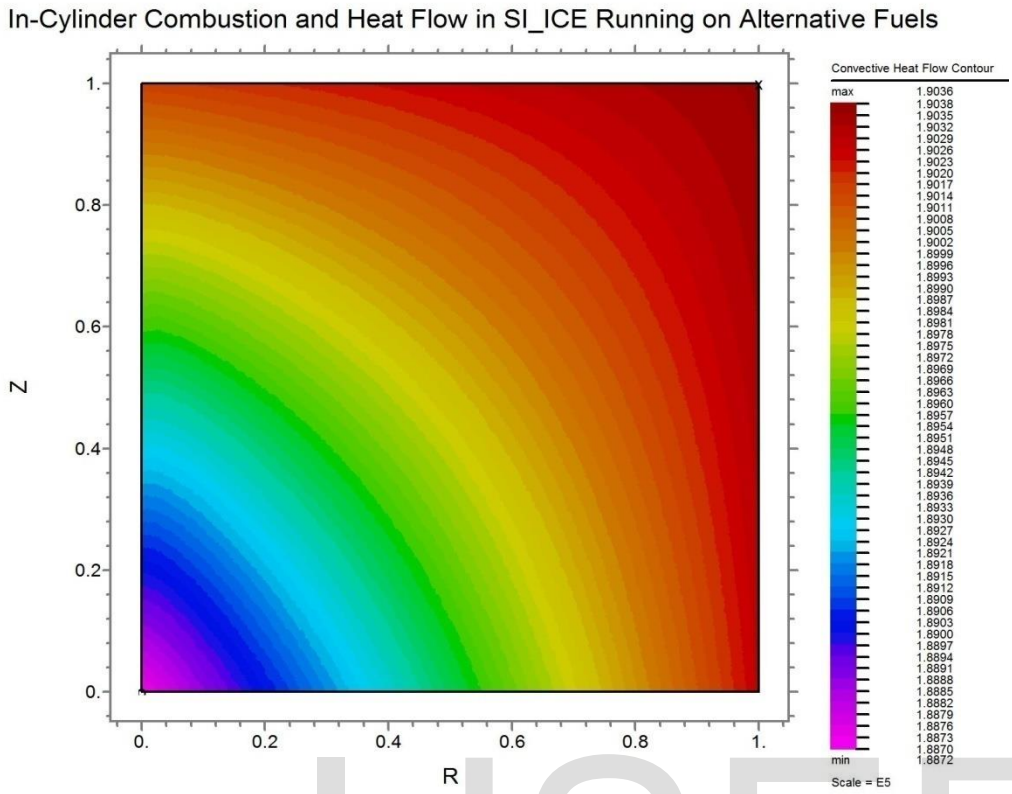

Fig 4b: Contour plot of in-cylinder convective heat flow for E20 blend

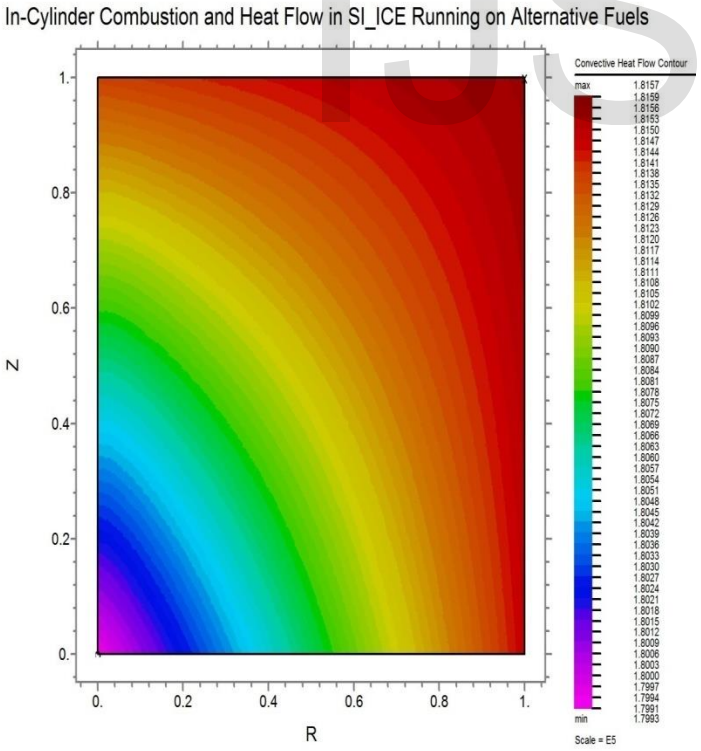

Fig 4c: Contour plot of in-cylinder convective heat flow for E30 blend

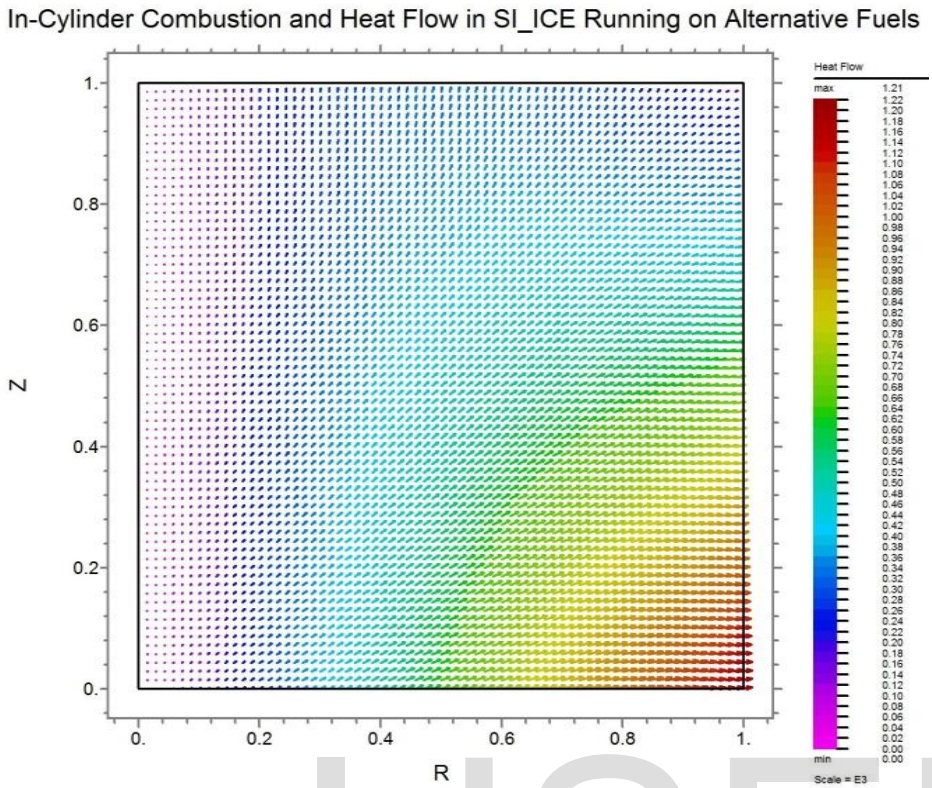

Fig 5a: Vector plot of in-cylinder conductive heat flow for E10 blend

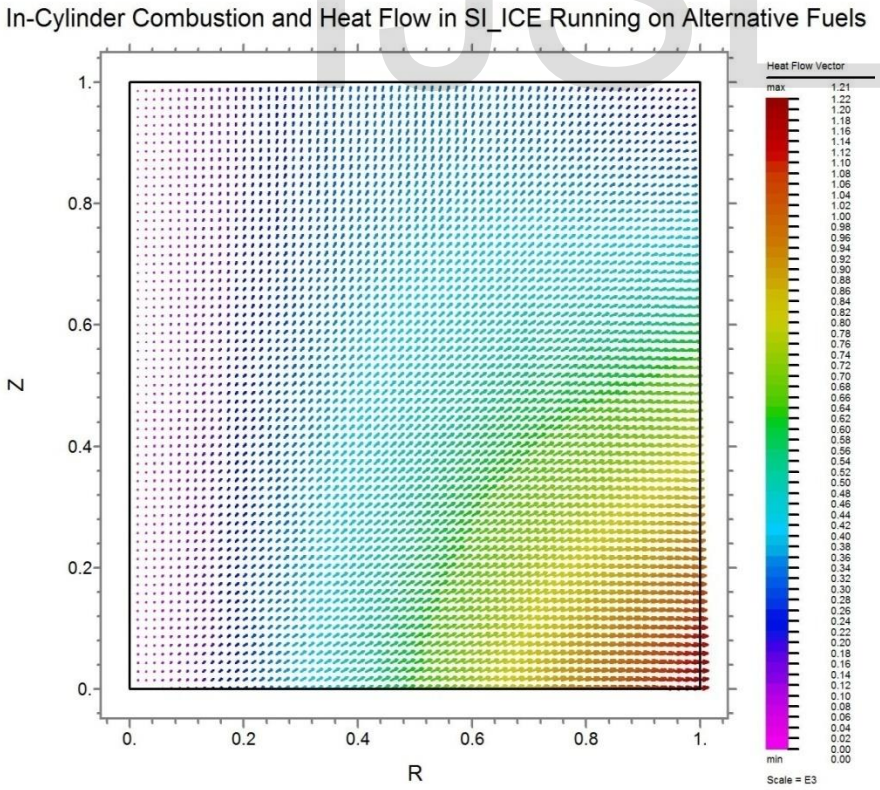

Fig 5b: Vector plot of in-cylinder conductive heat flow for E20 blend

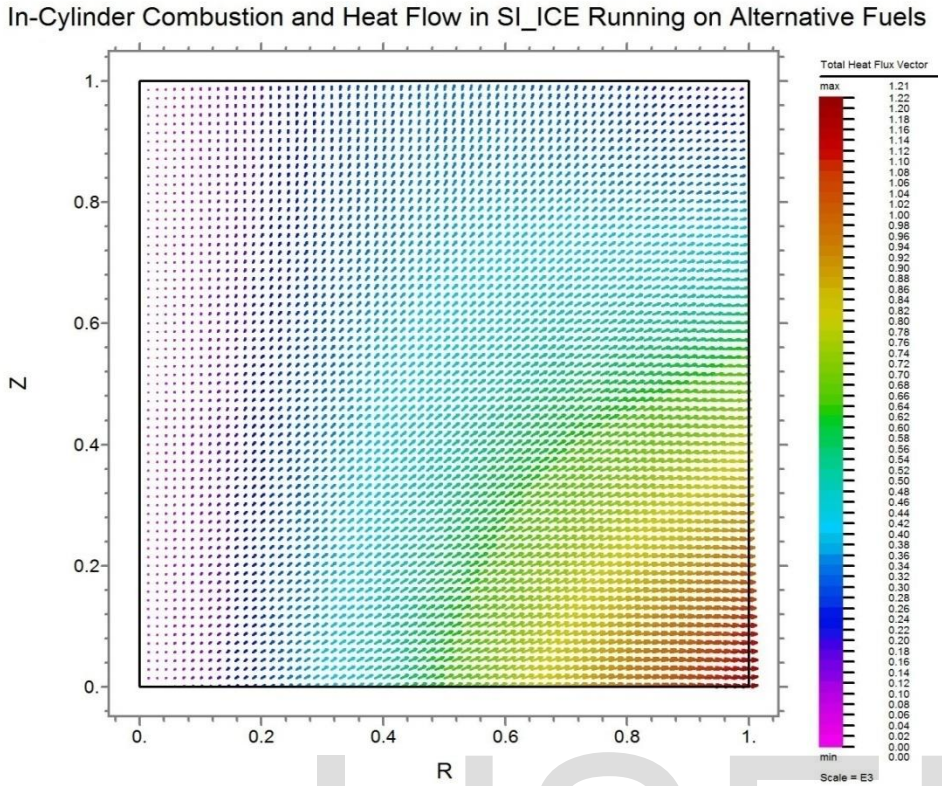

Fig 5c: Vector plot of in-cylinder conductive heat flow for E30 blend

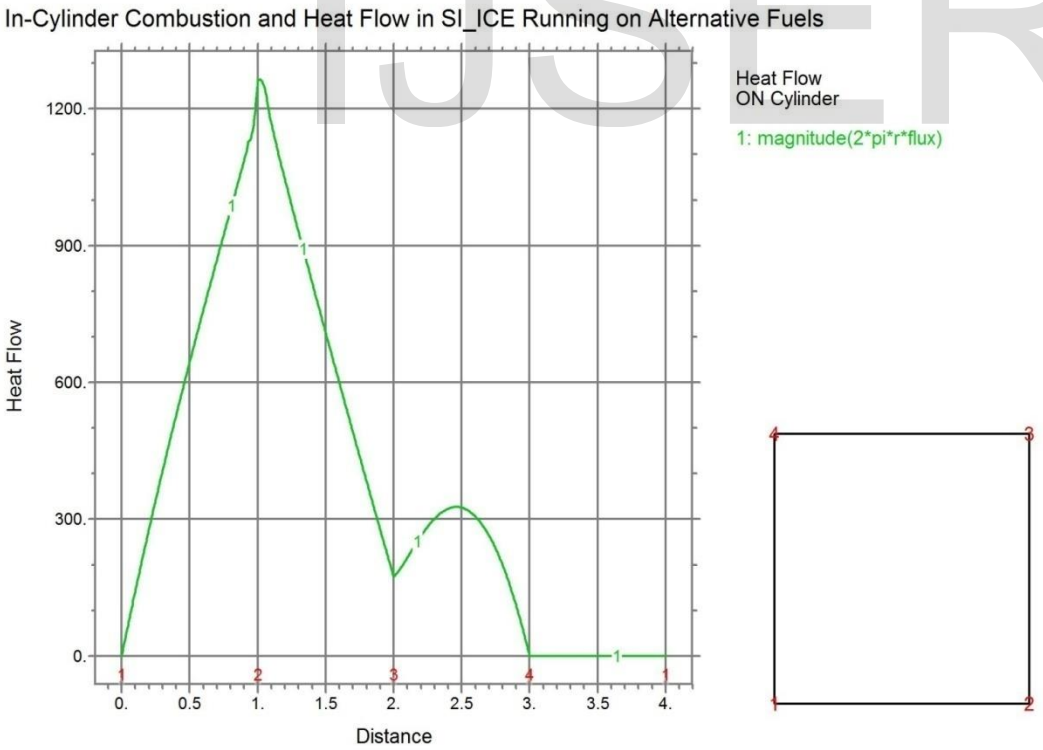

Fig 6: Elevation plot of heat flow on cylinder

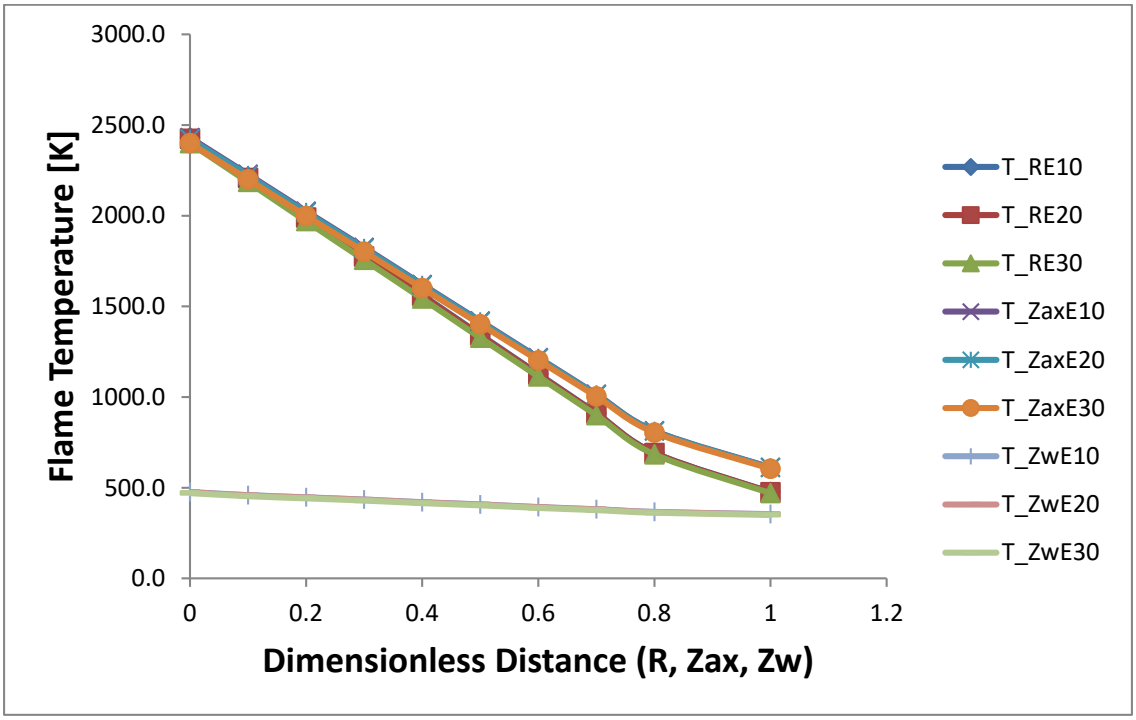

Fig 7: Flame temperature versus radial (R), axial (Zax) and wall (Zw) distances

Figs 1 and 2 show the contour and surface plots of normalized in-cylinder combustion temperature within the cylinder for E10, E20 and E30 blends. The flame developed following combustion is seen to be highly concentrated and intense around the top dead centre (TDC) and the flame front is observed to propagate in all directions towards the containing chamber walls and reciprocating piston head, and then extinguishes. Fig. 3 shows the heat flux in the cylinder for the three blends studied in 2-D radial and axial plane. It is common practice to treat turbulent flames as an array of laminar flamelets devoid of turbulence structure. Hence, the relaxation of turbulent combustion in this investigation and considering combustion as the rate of propagation of a flame through an ethanol-petrol fuel-and-oxidizer mixture with reference to a fixed cylinder content. The propagating flame results in swirl within the burning mixture, and consequently, the observed increased flux near TDC and near zero towards the bottom dead centre (BDC). Total heat flux is observed to be minimal axially down the chamber wall, primarily due to presence of hotspots at some parts of the cylinder wall. It is also minimal axially from the TDC to the piston head. There is no marked difference between the fluxes recorded for the given blends as 182, 182 and 180 W/m^2 for E10, E20 and E30, respectively.

Figs 4a, b and c present the convective heat transfer contours for the E10, E20 and E30 blends. The convective heat release ranges from 1.99-2.01*10^5, 1.89-1.90*10^5 and 1.80-1.82*10^5 W/m^2 for the E10, E20 and E30 blends, respectively. This reveals that as the volume of ethanol increases, the convective heat release decreases. It can be observed from the figures that the convective heat flow from the burning gases increases radially from the TDC, region of flame development to the chamber walls, also increases axially from TDC to the piston head, and as well increases diagonally from the TDC to the contact region between piston head and chamber wall. The heat flow rate is seen to be highest around the chamber wall and piston head. This increase in the heat transfer rate in the observed directions is as a result of the rapid distribution of temperature across and along the cylinder combustion space from the propagating burning mixtures. In spark-ignited engines, convective and conductive heat transfers are dominant since there is no particulate matter that radiates heat. These modes of heat loss remove energy from the combustion chamber and keep the cylinder walls from melting. Also, the presence of water jackets and coolants around the cylinder walls enable faster dissipation of heat from the burning gases to the chamber walls. It is to be noted that this effective heat transfer rate is needed to keep the cylinder walls from overheating, causing a decrease in exhaust temperature and knock tendency, improvement on the engine power output, brake torque and fuel economy.

Figs 5a, b and c show the vector plots of the total conductive heat flow in the R-Z plane of the engine cylinder for the E10, E20 and E30 blends respectively. Heat

transfer by conduction is concentrated around the top of the cylinder towards the wall from where it is conveyed to the gasket around the cylinder and crevices to the coolant, thus shielding the cylinder linings from adverse thermal stress. The maximum conductive heat release for all the three blends is in the region of 1.21 x 10^3 W/m^2. Fig. 6 depicts the elevation of heat flow around the cylinder. At the onset of combustion at point 1 (TDC) in the cylinder, conduction heat transfer increases rapidly towards the wall at point 2 where it is maximum. From point 2 at the wall, it decreases sharply to point 3 (BDC). Along the bottom dead centre, there is a fluctuation of heat conduction though not significant while it remained zero along the cylinder axis defined by line 4-1. It can be observed that the volume of ethanol in the blends does not have any pronounced effect on the conductive heat transfer in the cylinder.

Fig 7 shows the variation of flame temperature along normalized radial (R) and axial (Z) directions of the cylinder as well as the cylinder wall (Zw) for the E10, E20 and E30 blends. It can be observed that as the crank moves within the duration of combustion, adverse temperature gradient is very steep along the radial axis at TDC. Flame temperature is observed to be high at the point of start of ignition and decreases radially to the chamber wall. Along the axis of the cylinder, steep temperature gradient is also observed with a sharp decrease towards the BDC during combustion. Also, along the cylinder wall, the temperature variation is not significant, approximating to almost a constant value. This means that the engine block, cylinder head and piston crown of a modified engine that would run on petrol-ethanol blends should be strong enough to withstand high thermal stress as is evident in the current study.

4 Conclusion

A 2-D model of combustion and heat transfer in an axi-symmetric internal combustion engine has been developed. It has been used to simulate combustion and heat flow in an unmodified spark ignition engine running on three blends of ethanol and petrol, namely, E10, E20 and E30 blends. Steep temperature gradient was observed for the three blends with E10 having the highest flame temperature, highest heat flux and highest convective heat release while E30 recorded the least. Spatial temperature distribution as well as heat transfer in internal combustion engines running on alternative fuel such as ethanol-petrol blends is useful in the optimum sizing of the cooling system, engine component materials as well as emission reduction devices.

Acknowledgements

The financial supports provided at various times by the Federal University of Technology Owerri (FUTO) are gratefully acknowledged. The assistance and professional advice from Mr Marek Nelson of PDE Solutions Inc. USA is also gratefully acknowledged.

Nomenclature

A	Frequency factor of the reacting species in the combustion model
c_p	Specific heat capacity at constant pressure
E_a	Activation energy of the reacting species
h	Convective heat transfer coefficient
L	Connecting rod length
$\dot{m}$	Mass flow rate
N	Engine speed
Q	Fuel calorific value
R	Crank radius
R_u	Universal gas constant
$\dot{R}_f$	Rate of disappearance of unburned fuel mixture
S_p	Instantaneous piston speed
T_g	Gas temperature
T_w	Wall temperature
V_c	Clearance volume
V_s	Swept volume

Greek symbols

α	Thermal diffusivity

γ_v	Engine compression ratio
θ	Crank angle
κ	Thermal conductivity
μ	Dynamic viscosity
ρ	Density
$\dot{v}$	Kinematic viscosity
ω_f	Unburned fuel mass fraction
ω_{ox}	Unburned oxidizer mass fraction

References

[1] D. Turner, H. Xu, R.F. Cracknell, V. Natarajan, and X. Chen, "Combustion performance of bio-ethanol at various blend ratios in a gasoline direct injection engine", Fuel 90 (2011) 1999–2006.

[2] J.E. Tibaquirá, J.I. Huertas, S. Ospina, L.F. Quirama, and J.E. Niño, "The Effect of Using Ethanol-Gasoline Blends on the Mechanical, Energy and Environmental Performance of In-Use Vehicles", Energies 2018, 11, 221; doi:10.3390/en11010221.

[3] A. Mahmoud and A. Ahmed, "Investigation of Combustion Process of Single Fuel and Dual Fuel of Four Strokes Spark Ignition Engine", Journal of SAE, Volume 27, (2017).

[4] T. De Cuyper, K. Chana, M. De Paepe and S. Verhelst, "Heat Transfer Modelling in Spark Ignition Engines: Optimization and Instrumentation of a TGF Sensor", Osney Thermo-Fluids Laboratory, (2013).

[5] O. Spistov, "Modelling and Measurement of Local Heat Flux on the Cylinder of Compression Ignition IC Engine", International Journal of Research in Mechanical Engineering, Volume 1, Issue 4 (2013).

[6] P. Gustof and A. Hornik., "Determination of the Temperature Distribution in the Wet Cylinder Sleeve in Turbo Diesel Engine", Journal of Achievement in Materials and Manufacturing Engineering, Volume 27, Issue 2 (2008).

[7] M.A. Rivas Caicedo, E. Witrant, O. Sename, P. Higelin and C. Caillol, "Energy Wall Losses Estimation of a Gasoline Engine Using a Sliding Mode Observer", SAE 2012 World Congress & Exhibition, Apr 2012, Detroit, United States. pp.2012-01-0674, ⟨10.4271/2012-01-0674⟩. ⟨hal-00765566⟩.

[8] T.M. Belal, E.M. Marzouk and M.M. Osman, "Investigating Diesel Engine Performance and Emissions Using CFD", Energy and Power Engineering (2013)

[9] K.T. Ajayi and G.N. Nwaji, "Numerical Investigation of Internal Combustion Engine", International Journal of Engineering, Volume 4, No.2 (2010).

[10] O. C. Nwufo, C. F. Nwaiwu, C. Ononogbo, J. O. Igbokwe, O. M. I. Nwafor and E. E. Anyanwu "Performance, Emission and Combustion Characteristics of a Single Cylinder Spark Ignition Engine using Ethanol-Petrol Blended Fuels", International Journal of Ambient Energy, Volume 16, No. 5 (2017).

[11] K.T. Ajayi and G.N. Nwaji, "Numerical Simulation of Combustion with Multi-Dimensional Flame Propagation in Axisymmetric Internal Combustion Engine", NIMechE International Conference, (2011), 8-18.

[12] J.B. Heywood, "Internal Combustion Engine Fundamentals", McGraw-Hill Inc., New York, (1988).

[13] Richard Stone, "Introduction to Internal Combustion Engines", Second Edition, MacMillan Press Ltd, (1992)

[14] P.S. Gill, "A Textbook of Automobile Engineering, Volume 1, Granit Hillside, MacMillan Press Ltd , 2012.

[15] A.F. Kheiralla, M.M. El-Awad, M.Y. Hassan, M.A. Hussen and I. Hind, "Experimental Determination of Fuel Properties of Ethanol/Gasoline Blends as Bio-fuel for SI engines", International Conference on Mechanical, Automobile and Robotics Engineering, Penang (2012), 244-249.

[16] R.S. Turns, "An Introduction to Combustion: Concepts and Applications", Second Edition, McGraw-Hills Inc., New York, 2000.

[17] M.U. Warnatz and R.W. Dibble, "Combustion: Physical and Chemical Fundamentals, Modelling and Simulation, Experiments, Pollutant Formation", 4th Edition, Springer, 2006.

[18] T.B. Alrayyes, "The Effect of Ethanol on Combustion Characteristics of Spray Guided Direct Injection Spark Ignition Engine", IUG Journal of Natural and Engineering Studies, Vol 24, No 1, (2016), 26-38.